Iranian Journal of Catalysis 5(1), 2015, 49-56

IRANIAN JOURNAL OF CATALYSIS

Fe_3O_4/FDU-12: A Highly Efficient and Magnetically Separable Nano-Catalyst for Oxidation of Alcohols

Najme Kalvari Janaki, Razieh Fazaeli*, Hamid Aliyan

Department of Chemistry, Shahreza Branch, Islamic Azad University, 86145-311, Iran.

Received 4 August 2014; received in revised form 17 September 2014; accepted 6 October 2014

ABSTRACT

A series of Fe_3O_4 supported on mesoporous FDU-12 silica systems were prepared by the hydrothermal conditions. The surface properties of the functionalized catalyst were analyzed by a series of characterization techniques like FTIR, XRD, N_2 adsorption–desorption and TEM. XRD and adsorption–desorption analysis shows that the mesostructure of FDU silica remains intact after Fe_3O_4 modifications, while spectral technique show the successful immobilizing of the neat Fe_3O_4 inside the porous silica support. Fe_3O_4/FDU-12 system, has emerged as highly efficient and magnetically recoverable heterogeneous catalyst for selective oxidation of alcohols with H_2O_2 at reflux conditions because of its high specific surface area, tuneable pore size, and unique structure. The advantages of this catalytic system is mild reaction conditions, short reaction times, high product yields, easy preparation of the catalysts, non-toxicity of the catalysts, simple and clean work-up of the desired products. The wet catalyst can be removed easily, recovered and reused without significant loss of activity.

Keywords: *Mesoporous FDU-12; Fe_3O_4 NP; Nanocomposite; Heterogeneous catalysis.*

1. Introduction

Since ordered mesoporous silicas, KSW-1 [1] and MCM-41 [2,3], were reported for the first time in the 1990s, many other mesoporous silicas with various pore geometries, such as MCM-48 [3,4], SBA-15 [5,6], SBA-16 [6–8], KIT-6 [9] and FDU-12 [10,11], have been synthesized and characterized chiefly by low-angle powder X-ray diffraction (XRD), transmission electron microscopy (TEM) and N_2 adsorption/desorption. The most important characteristics of the mesoporous silicas are the large surface area, high mesopore volume, and narrow pore size distribution in the range of mesopores. However, many applications (such as adsorption, ion exchange, catalysis and sensing) require these silica-based materials to have specific attributes such as binding sites, stereochemical configuration, charge density and acidity [12]. Functionalization of the silica surface with organic groups is very important and can be achieved via post synthesis grafting or direct co-condensation synthesis routes [13,14].

FDU-12 consists of spherical nanocavities linked together by some very short nanochannels or windows [15-17]. FDU-12 is face-centred cubic (space group Fm3m). The pore sizes of FDU-12 are normally about 10–12.3 nm in diameter. It is possible to increase the pore size up to 27 nm in FDU-12 with a hydrothermal treatment at 15ºC [18], and the size of the entrances joining two adjacent cavities can be tuned in the range of 4–9 nm in diameter using different maturation temperatures in a range from 100 to 140 °C.

On the other hand, iron oxide nanomaterials have been extensively studied by material researchers in recent years, due to their novel physicochemical properties and advantages (high saturation magnetization, easy synthesis, low cost, etc.) and wide applications in many fields (magnetic recording, pigment, magnetic separation, and magnetic resonance imaging, MRI) [19-24].

Encapsulating magnetic nanoparticles in silica is a promising and important approach in the development of magnetic nanoparticles for technological and biomedical applications [25,26]. Materials used in these ways can be defined as magnetisable particles (i.e. ones that, when under the influence of an external magnetic field, will themselves become magnetic) and can enable the isolation or extraction of a target molecule or substance. The non-magnetic target binds to the surface of the magnetisable solid-phase support

---

*Corresponding author email: fazaeli@iaush.ac.ir
Tel: +98 31 53502706-7; Fax: 031 53502701-2

(MSPS), either through a specific affinity interaction, or another mechanism, for example, ion exchange or hydrophobic interaction, so that it can then be isolated or extracted by application of an external magnetic field [27].

Herein, we report on the catalytic behavior of Fe_3O_4/FDU-12 catalysts (fabricated via the encapsulated methods) for the oxidation of alcohols using H_2O_2 (Scheme 1).

2. Experimental

2.1. General

All materials were commercial reagent grade. Infrared spectra (400–4000 cm^{-1}) were recorded from KBr pellets on a PerkinElmer Spectrum 65 spectrometer. The X-ray powdered diffraction patterns were performed on a Bruker-D8ADVANCE with automatic control. The patterns were run with monochromatic Cu Kα (1.5406 Å) radiation with a scan rate of 2° min^{-1}. Nitrogen adsorption measurements were performed at −196 ◦C by using an ASAP 2010M surface analyzer, and the pretreatment temperature was 180 ◦C. Transmission electron micrographs (TEM) were obtained on a Joel JEM 2010 scan-transmission electron microscope. The sample for the TEM measurement was suspended in ethanol and supported on a carbon coated copper grid.

2.2. Synthesis of Fe_3O_4/FDU-12

Cage-containing mesoporous silica, FDU-12, were synthesized according to the corresponding literature [10, 11]. The magnetic Fe_3O_4 nanoparticles (NPs) were prepared through a solvothermal reaction. $FeCl_3\cdot 6H_2O$ (1.35 g) and sodium acetate (3.6 g) were dissolved in ethylene glycol (40 mL) under magnetic stirring. The obtained homogeneous yellow solution was transferred to a teflon-lined stainless-steel autoclave and sealed for heating at 200 ºC. After a reaction time of 8 h, the autoclave was cooled to room temperature. The obtained black magnetite particles were washed with ethanol six times and then dried in vacuum at 60 ºC for 12 h. The Fe_3O_4-supported FDU-12 catalyst was prepared by method of hydrothermal conditions: mixing 50 mg of Fe_3O_4 and 100 mg of the FDU-12 sample with 10 mL of distilled water in an autoclave Teflon container under static conditions at 493 K for 8 h.

2.3. Oxidation of alcohols, general procedure

A 10-ml round bottomed flask with 5 ml of H_2O equipped with a mechanical stirrer and reflux condenser was charged with Fe_3O_4/FDU-12 catalyst (0.015 g, 2 mmol) and aqueous hydrogen peroxide (30 %) (3 mmol). The mixture was stirred for 15 minutes followed by addition of an alcohol (1 mmol) was added. The biphasic mixture was stirred at 80ºC for the required time. Progress of the reaction was followed by the aliquots withdrawn directly from the reaction mixture analysed by GC using internal standard. After completion of the reaction, the Fe_3O_4/FDU-12 catalyst was removed by applying a magnetic field. The reaction mixture was then treated with a 10 % sodium hydrogen sulfite solution (15 ml) to decompose the unreacted hydrogen peroxide followed by treatment with 10 % sodium hydroxide (20 ml). The product was extracted with *n*-butyl-ether. The pure product was obtained by distillation or silica gel column chromatography (hexane/ ethyl acetate, 10/1).

3. Results and Discussion

3.1. Physico-chemical characterization

FT-IR spectra of FDU-12 and Fe_3O_4/FDU-12 are shown in Fig. 1. As shown in the spectrum of the parent FDU-12 silica, the typical bands due to siliceous Si–O–Si material are observed: A main band at 1094 cm^{-1} with a shoulder at 1265 cm^{-1}, due to asymmetric Si–O–Si stretching modes, the corresponding symmetric stretch at 814 cm^{-1} [28]. FT-IR analysis reveals that Fe_3O_4/FDU-12 nanocomposites (Fig. 1b) have characteristics peaks at around at 1625, 1091, 815, 471 cm^{-1} for FDU-12. The peak at 560 cm^{-1} could be attributed to the Fe-O stretching of Fe_3O_4.

The XRD patterns of Fe_3O_4/FDU-12 (Fig. 2) reveal that the crystal structure is indexed as face centered cubic (fcc). It is found that the strong diffraction peaks situated at 2θ of 18.900, 30.220, 35.530, 43.240, 53.970, 57.440, and 62.940, corresponding to the diffractions of [111], [220], [311], [400], [422], [511], and [440] crystal faces of Fe_3O_4 structures. Sharp peaks in Fig. 2 suggest that the Fe_3O_4/FDU-12 nanocomposite have good crystalline abilities. The average crystal sizes calculated from the XRD patterns according to Scherrer formula is 3.8 nm for the Fe_3O_4/FDU-12.

The maintenance of the FDU-12 frameworks after introduction of Fe_3O_4 is further supported by the nitrogen sorption data. Nitrogen adsorption isotherm for the calcined FDU-12 sample is shown in Fig. 3a. The FDU-12 sample exhibited adsorption isotherm with broad adsorption–desorption hysteresis loop [29]. Fig. 3b shows the N_2 adsorption–desorption isotherms and pore size distributions of Fe_3O_4/FDU-12.

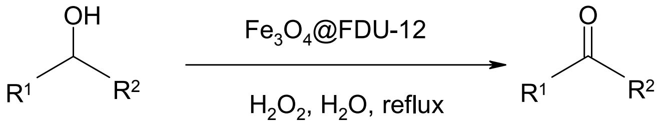

Scheme 1. Oxidation of alcohols with H_2O_2 in the presence of Fe_3O_4@ FDU-12.

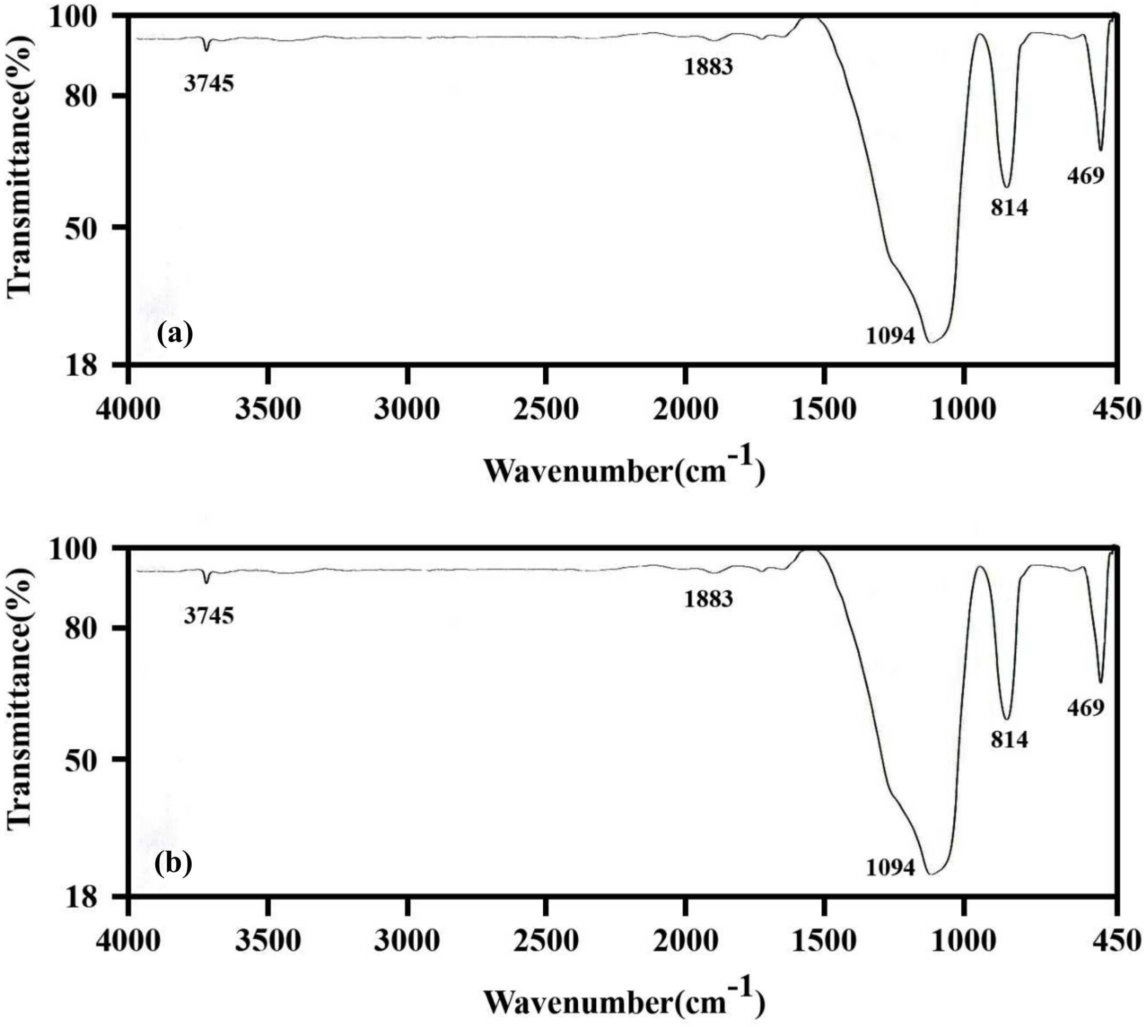

Fig. 1. FTIR spectra of (a) FDU-12 and (b) Fe_3O_4/FDU-12.

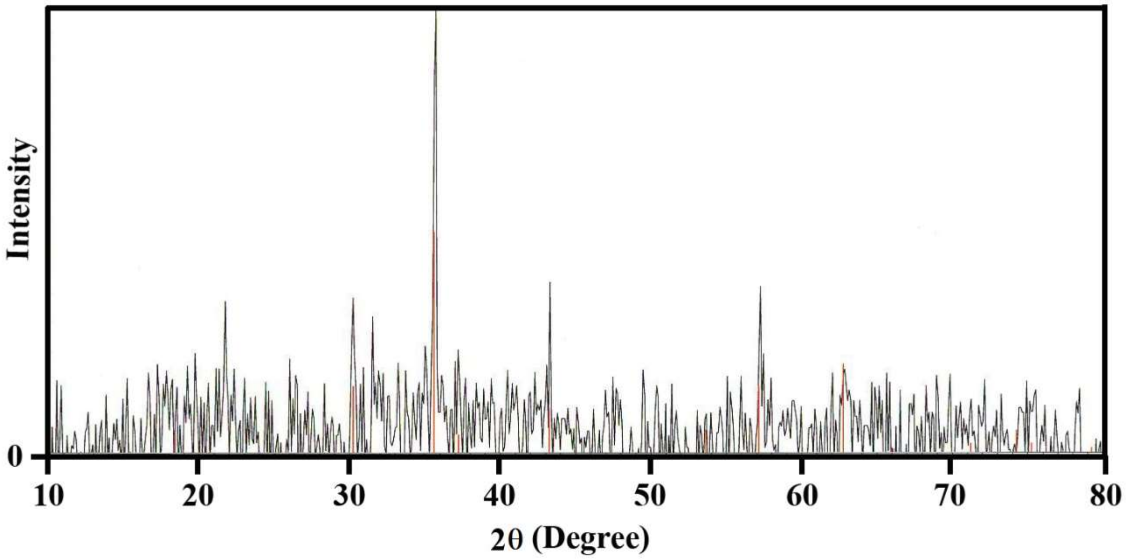

Fig. 2. XRD patterns of Fe_3O_4/FDU-12.

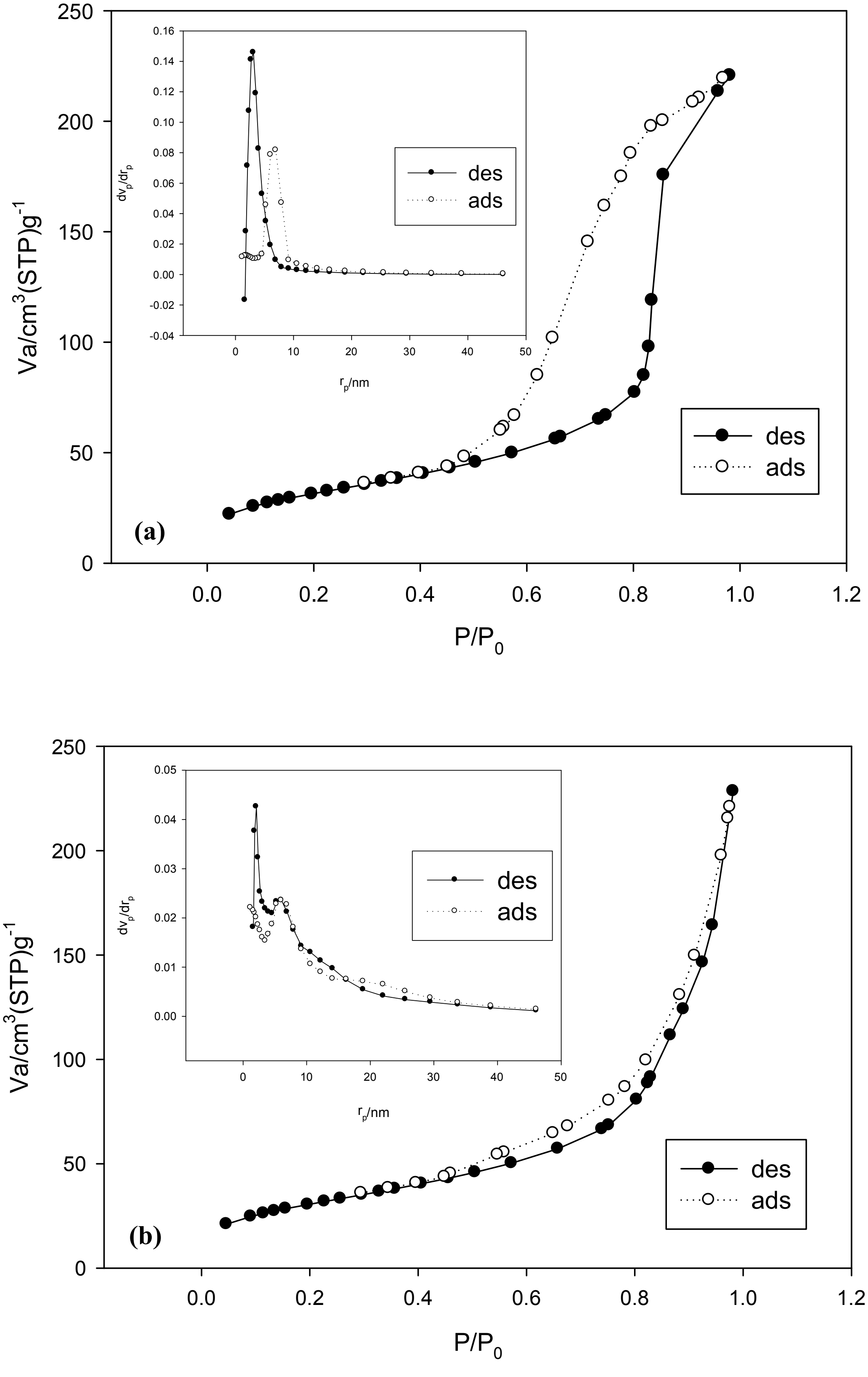

Fig. 3. N_2-adsorption-desorption isotherms of (a) FDU-12 and (b) Fe_3O_4@FDU-12: (inset) pore size distributions calculated by the Barrett-Joyner-Halenda (BJH) method

The samples exhibited typical IV type isotherms and H1 type hysteresis loops at high relative pressures. The pore size distribution of the sample is shown in the inset of Fig. 3. Interestingly, the Fe_3O_4/FDU-12 showed very similar isotherm patterns and pore size distributions (inset) compared to those of FDU-12, indicating that the structure of FDU-12 was still maintained even after the immobilizing step of Fe_3O_4.

Structural properties of FDU-12 are listed in Table 1. FDU-12 showed BET surface area of 1760 m^2/g and pore volume of 0.75 cm^3/g. After Fe_3O_4 modification, the nitrogen adsorption isotherm became an even line and the volume adsorbed decreased distinctly, suggesting the occupation of the pore by Fe_3O_4. BET surface area and pore volume of Fe_3O_4@FDU-12 decreased which confirms that Fe_3O_4 have occupied the channels in FDU-12.

The TEM images of the Fe_3O_4/FDU-12 sample are shown in Fig. 4. From these images the distribution of Fe_3O_4 nanocrystals in mesoporous matrix can be observed clearly. TEM analyses indicates that the continuous 3D pore structure of the FDU-12 is robust enough to survive the Fe_3O_4 incorporation process and so offers an excellent matrix to support highly dispersed Fe_3O_4 species. The places with darker contrast could be assigned to the presence of Fe_3O_4 particles with different dispersion. The small dark spots in the images could be ascribed to Fe_3O_4 particles, probably located in to the FDU-12 cavities. The larger dark areas over the cavities most likely correspond to Fe_3O_4 agglomerates on the external surface. The specimen seems to have some clusters of nanocrystallites without any ordering.

3.2. Catalytic activity

3.2.1. Oxidation of alcohols

As summarized in Table 2, benzylic and allylic alcohols are generally excellent substrates for this catalyst with electron-rich alcohols having the fastest reaction rates. Comparing benzyl alcohols to benzylic alcohols with electron-releasing substituents (Table 1, Entry 1-6), we found that the reaction time for electron-rich benzylic alcohols (Table 1, Entry 2) were shorter.

The successful oxidation of benzoin and furfuryl alcohol as model substrates shows a superior capability of Fe_3O_4/FDU-12 in oxidizing similar substrates

Table 1. The texture parameters of FDU-12 and Fe_3O_4 modified FDU-12 in comparison with the bulk Fe_3O_4 materials.

Materials	Texture parameters (N_2 adsorption)			Fe_3O_4 (wt%)[b]	FDU-12
	Surface area (m^2/g)[a]	Pore volume (cm^3/g)[a]	Pore diameter (nm)		
FDU-12	1760	0.75	2.3	-	100
Fe_3O_4	4	0.01	11.7	100	-
Fe_3O_4@ FDU-12	533	0.38	1.47	28.1±0.8	71.9±0.8

[a] Total pore volume measured at $p/p_0 = 0.99$.

[b] The average results of atomic adsorption analysis, NAA and ICP.

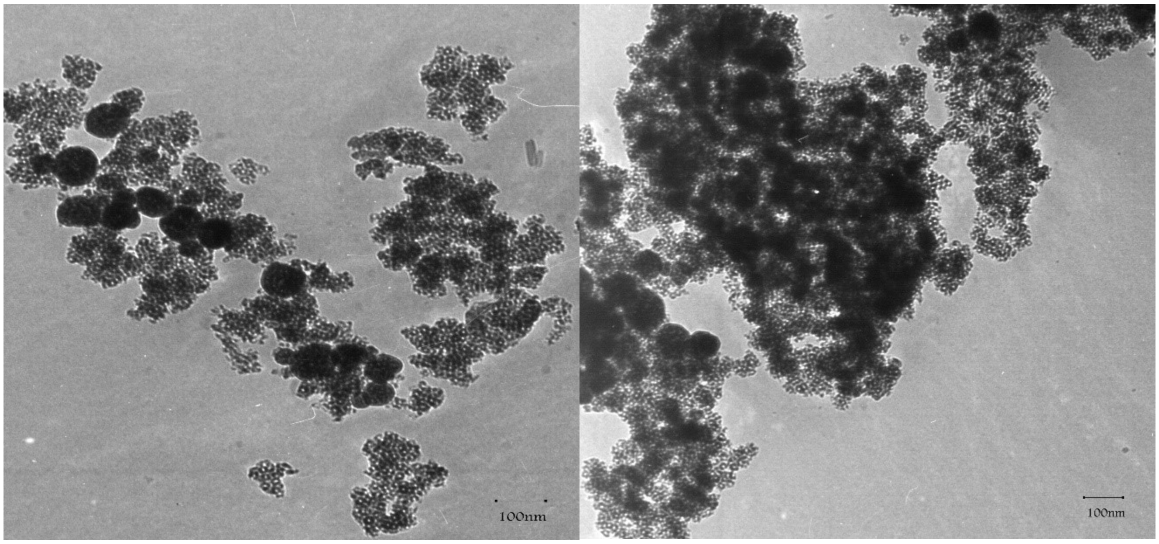

Fig. 4. TEM image for Fe_3O_4/FDU-12.

(Table 2, entries 7, 11). Catalyst Fe_3O_4/FDU-12 in particular showed excellent reactivity for the selective oxidation of various types of allylic alcohols yielding the corresponding *α,β*-unsaturated carbonyl compounds in excellent yields (Table 2, entries 12–15). It is worth mentioning that in the oxidation of allylic alcohols, C=C double bonds remained intact without an intramolecular hydrogen transfer. Secondary benzylic alcohols were also efficiently oxidized into the corresponding ketone (Table 2, entries 8-11). Unfortunately, using Fe_3O_4/FDU-12, aliphatic alcohols such as 1-octanol and 2-octanol and 4-phenyl cyclohexanol were less reactive (Table 2, entries 16-18) and lower conversions and yields were observed even after prolonged reaction time. The catalytic system shows high selectivity, and only a trace amount of acid (below 1%) was formed.

In order to show the merit of the present work in comparison with recently reported protocols [30-36], we compared the results with respect to the amounts of the catalysts used, reaction times and yields of the products (Table 3). Comparison of Fe_3O_4@FDU-12 with these catalysts for selective oxidation of alcohols show that activity of Fe_3O_4@FDU-12 seems to be higher than or equal with other known catalysts.

3.2.2. Recovery

Magnetic separation provides a very convenient approach for removing and recycling magnetic composites. The separation of Fe_3O_4/FDU-12 nanocatalyst from the reaction mixture becomes very easy owing to the super paramagnetic nature of Fe_3O_4 nanoparticles at room temperature. In the magnetic separation technique, the catalyst became adsorbed onto the magnetic stirring bar when the stirring was stopped. In our experiments, the reusability of the catalyst was examined by repetitive use of the catalyst. A catalyst recycle experiment (1 mmol of benzyl alcohol, 3 mmol of H_2O_2, reflux in H_2O (3 ml), 1 h) carried out simply by magnetic separation of catalyst and re-addition of benzyl alcohol (1 mmol) showed 98%, 98%, and 96% yields in three reaction cycles with benzaldehyde as the only product.

4. Conclusions

A series of Fe_3O_4/FDU-12 catalysts were prepared by the wet impregnation method. This catalyst is a safe and magnetically recoverable heterogeneous system for promoting the highly chemoselective and rapid oxidation of alcohols to aldehydes with H_2O_2. The advantages of this catalytic system is mild reaction conditions, short reaction times, high product yields, easy preparation of the catalysts, non-toxicity of the catalysts, simple and clean work-up of the desired products.

Acknowledgements

We gratefully thank Shahreza Branch, Islamic Azad University, for financial support.

References

[1] T. Yanagisawa, T. Shimizu, K. Kuroda, Bull. Chem. Soc. Jpn. 63 (1990) 988–992.

[2] C.T. Kresge, M.E. Leonowicz, W.J. Roth, Nature 359 (1992) 710–712.

[3] J.S. Beck, J.C. Vartuli, W.J. Roth, J. Am. Chem. Soc. 114 (1992) 10834–10843.

[4] A. Monnier, F. Schuth, Q. Huo, Science 261 (1993) 1299–1303.

[5] D.Y. Zhao, J.L. Feng, Q.S. Huo, Science 279 (1998) 548–552.

[6] D.Y. Zhao, Q.S. Huo, J.L. Feng, J. Am. Chem .Soc. 120 (1998) 6024–6036.

[7] Y. Sakamoto, M. Kaneda, O. Terasaki, Nature 408 (2000) 449–453.

[8] P.I. Ravikovitch, A.V. Neimark, Langmuir 18 (2002) 9830–9837.

[9] F. Kleitz, S.H. Choi, R. Ryoo, R. Chem. Commun. (2003) 2136–2137.

[10] J. Fan, C.Z. Yu, T. Gao, T. Angew. Chem. Int. Ed. 42 (2003) 3146–3150.

[11] J. Fan, C.Z. Yu, J. Lei, J. Am. Chem. Soc. 127 (2005) 10794–10795.

[12] R.K. Dey, F.J.V.E. Oliveira, C. Airoldi, Colloid Surf. A 324 (2008) 41–46.

[13] X. Feng, G.E. Fryxell, L.O. Wang, A.Y. Kim, J. Liu, K.M. Kemner, Science 276 (1997) 923–926.

[14] M.H. Lim, A. Stein, Chem. Mater. 11 (1999) 3285–3295.

[15] D.Y. Zhao, Q.S. Huo, J.L. Feng, B.F. Chmelka, G.D. Stucky, J. Am. Chem. Soc. 120 (1998) 6024–6036.

[16] Y. Sakamoto, M. Kaneda, O. Terasaki, D.Y. Zhao, J.M. Kim, G. Stucky, H.J. Shim, R. Ryoo, Nature 408 (2000) 449–53.

[17] J. Fan, C.Z. Yu, T. Gao, J. Lei, B.Z. Tian, L.M. Wang, Q. Luo, B. Tu,. W.Z. Zhou, D.Y. Zhao, Angew. Chem. Int. Ed. 42 (2003) 3146–3150.

[18] J. Fan, C.Z. Yu, J. Lei, Q. Zhang, T.C. Li, B. Tu, W.Z. Zhou, D.Y. Zhao, J. Am. Chem. Soc. 127 (2005) 10794–10795.

[19] W. Wu, X.H. Xiao, S.F. Zhang, H. Li X.D. Zhou, C.Z. Jiang, Res. Lett. 4 (2009) 926.

[20] M. Faraji, Y. Yamini, M. Rezaee, J. Iran Chem. Soc. 7 (2010) 1-37.

[21] P. Landon, J. Ferguson, B.E. Solsona, T. Garcia, S. Al-Sayari, A.F. Carley, A.A. Herzing, C.J. Kiely, M. Makkee , J.A. Moulijn, A. Overweg, S.E. Golunski, G.J. Hutchings, J. Mater. Chem. 16 (2006) 199-208.

[22] Y. Wang, Y.M. Wang, J.L. Cao, F.H. Kong , H.J. Xia , J. Zhang, B.L. Zhu, S.R. Wang, S.H. Wu, Sensors Actuat. B: Chem. 131 (2008) 183-189.

[23] Z. Zhong, J. Ho, J. Teo, S. Shen, S.A. Gedanken, Chem. Mater. 19 (2007) 4776-4782.

Table 2. Oxidation of alcohols by Fe_3O_4/FDU-12 in CH_3CN with H_2O_2[a].

Entry	Substrate	Product	Time (h) : Yield (%)[b]
1	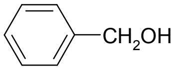	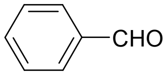	1:98
2	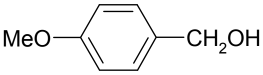	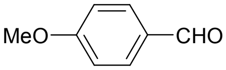	1.8: 95
3	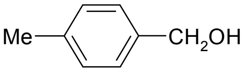	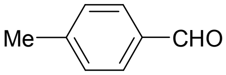	3.5: 90
4	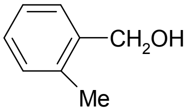	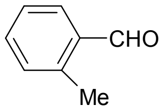	3:80
5	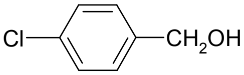	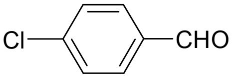	4:87
6	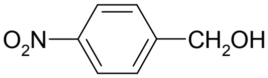	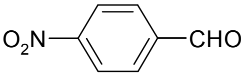	3:95
7	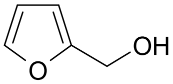	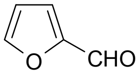	5:90
8	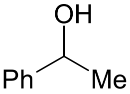	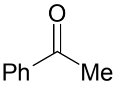	4: 90
9	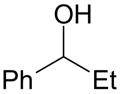	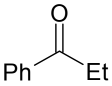	3.5 : 92
10	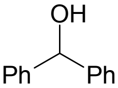	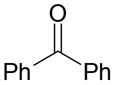	6.5:87
11	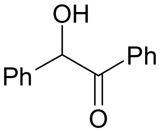	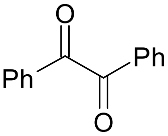	5.5:90
12	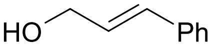	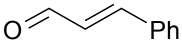	7:92
13	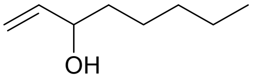	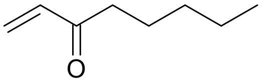	12: 95
14	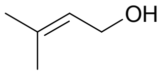	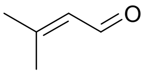	8:92
15	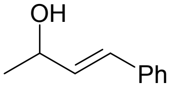	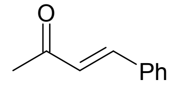	13:92
16	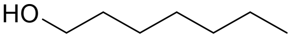	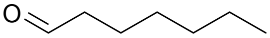	12:43[c]
17	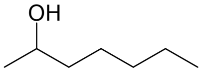	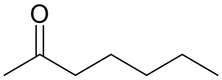	15: 48
18	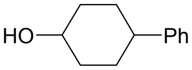	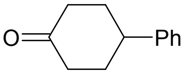	17: 40

[a] Reaction conditions: alcohol (1 mmol); H_2O_2 (3 mmol); Fe_3O_4@ FDU-12 (0.015 g, 2 mmol); reflux in H_2O (3 ml).

[b] GC yield based on an internal standard methods unless otherwise stated.

[c] A trace amount of the corresponding esters (~ 7 %) and carboxylic acid (~ 12%) were formed.

Table 3. Comparison of Fe_3O_4/FDU-12 with some other catalyst for oxidation of $PhCH_2OH$.

Entry	Reagent	Conditions	Time (h)	Conversion (%)	Yield (%)[a]	Ref.
1	Iron Chloride Hexahydrate/TEMPO (4 mol%)	O_2, Toluene, 80 °C	7	100	98	[30]
2	Au_{24} Clusters (Pd)/(CNT)[d] (50 mg)	O_2, 30 °C	6	74	24:53[b]:23[c]	[31]
3	Immobilized Pd, KNO_3 (4 mol%)	O_2, TFT, reflux	1.5	100	98	[32]
4	Polyester based Pd(II) Macrocomplexes (4 mol%)	Toluene, 70 °C	18	59	-	[33]
5	Hemicryptophane-Ruthenium Complex (5 mol%)	$CH_3CN:H_2O$, r.t.	1	-	91:9[b]	[34]
6	Liquid phase/Au NPpore (10 mol%)	O_2, MeOH, 60 °C	24		85	[35]
7	Triple-site phosphotungstate (5 mol%)	Toluene/H_2O_2, 90 °C	1		92	[36]
8	Fe_3O_4@FDU-12 (2 mol%)	CH_3CN, H_2O_2, reflux	1		98	This work

[a] Yield refers to the corresponding aldehyde.
[b] Yield refers to the corresponding acid.
[c] Yield refers to the benzoate.
[d] CNT is carbon nanotube.

[24] U.I. Tromsdorf, N.C. Bigall, M.G. Kaul, O.T. Bruns, M.S. Nikolic, B. Mollwitz, R.A. Sperling, R. Reimer, H. Hohenberg, W.J. Parak, S. Forster, U. Beisiegel, G. Adam, H. Weller, Nano Lett. 7 (2007) 2422-2427.

[25] L. Levy, Y. Sahoo, K. S. Kim, E.J. Bergey, P.N. Prasad, Chem. Mater. 14 (2002) 3715-3721.

[26] R. Arundhathi, D. Damodara, P.R. Likhar, M.L. Kantam, P. Saravanan, T. Magdaleno, S.H. Kwon, Adv. Synth. Catal. 353 (2011) 1591–1600.

[27] P.J. Robinson, P. Dunnill, M.D. Lilly, Biotechnol. Bioeng. 15 (1973) 603-606.

[28] H. Li, F. Zhang, H. Yin, Y. Wan, Y. Lu, Green Chem. 9 (2007) 500–505.

[29] M. Kruk, C.M. Hui, Microporous Mesoporous Mater. 114 (2008) 64–73.

[30] L.Wang, J. Li, Y. Lv, G. Zhao, S. Gao, Appl. Organometal. Chem. 26 (2012) 37–43.

[31] S. Xie, H. Tsunoyama, W. Kurashige, Y. Negishi, T. Tsukuda, ACS Catal. 2 (2012) 1519−1523.

[32] B. Karimi, A. Zamani, S. Abedi, J. H. Clark, Green Chem. 11 (2009)109–119.

[33] G. Giachi, M. Frediani, W. Oberhauser, E. Passaglia, J. Polymer Sci. A: Polymer Chem. 50 (2012) 2725–2731.

[34] Y. Makita, T. Fujita, T. Danno, M. Inoue, M. Ueshima, S.-I. Fujiwara, A. Ogawa, Supramolecular Catal. (2012) 9-11.

[35] N. Asao, N. Hatakeyam, M., T. Minato, E. Ito, M. Hara, Y. Kim, Y. Yamamoto, M. Chen, W. Zhangi, A. Inouei, Chem. Commun. 48 (2012) 4540–4542.

[36] Y. He, X. Ma, M. Lu, ARKIVOC VIII (2012) 187-197.